

Robust Strong Lensing Time Delay Estimation

Alireza Hojjati¹, Alex G. Kim², Eric V. Linder^{1,2,3}

¹*Institute for the Early Universe WCU, Ewha Womans University, Seoul 120-750, Korea*

²*Lawrence Berkeley National Laboratory, Berkeley, CA 94720, USA*

³*Berkeley Center for Cosmological Physics, University of California, Berkeley, CA 94720, USA*

(Dated: December 2, 2024)

Strong gravitational lensing of time variable sources such as quasars and supernovae creates observable time delays between the multiple images. Time delays can provide a powerful cosmographic probe through the “time delay distance” involving the ratio of lens, source, and lens-source distances. However, lightcurves of lensed images have measurement gaps, noise, systematics such as microlensing from substructure along an image line of sight, and no a priori functional model, making robust time delay estimation challenging. Using Gaussian process techniques, we demonstrate success in accurate blind reconstruction of time delays and reduction in uncertainties for real data.

I. INTRODUCTION

Multiple images of a single source are dramatic evidence for the effect of gravity, specifically general relativity, on light. This strong gravitational lensing not only splits the images, but magnifies or demagnifies the source flux and induces time delays between the images. The time delays arise from both the geometric path differences along the various lines of sight and the gravitational potential differences traversed by the photons.

When the source is variable, such as from a quasar or supernova, the time delays in the flux of one image relative to another can be observed. With careful modeling of the lens mass distribution, and measurement of the angular positions of the images, the geometric factors of distances between observer and lens, observer and source, and lens and source can be extracted as a ratio called the time delay distance. Recent advances in lens modeling [1, 2] and careful, long term flux monitoring programs such as CosmoGrail [3] (also see [4, 5]) have matured strong lensing time delays to an incipient cosmographic probe.

This prospect is exciting for several reasons. Since time delays over cosmological distances are sensitive not just to the overall scale, or Hubble constant, but the cosmic energy density and its evolution with redshift, one can constrain (combinations of) the matter and dark energy densities and dark energy equation of state. Moreover, the time delay distance acts fundamentally differently from luminosity and angular distances measured by calibrated standard candles such as Type Ia supernovae and rulers such as baryon acoustic oscillations. Hence it has distinct covariances among cosmological parameters and can be powerful in complementarity with the standard distance probes [6, 7]. Finally, despite the lens mass modeling, strong lensing time delays are a geometric probe and are tied only to the late universe, unique except for supernovae (but with different systematics and covariances) among all cosmological probes.

Here we address one important element of the use of lensing time delays: accurate estimation of the actual time delays. While great progress has been made in recent years (see, e.g., [8–10]), in large part due to heroic

observing programs and improved data sets, this is not a solved problem. Mathematically, one can consider it as reconstructing a shift between multiple noisy, irregularly sampled, differentially amplified data streams. We apply a special combination of Gaussian process statistics to this task. Such a concept for strong lensing dates back to [11] and more recently has been shown to have reasonable success [8]; we introduce several new features that exhibit noticeable improvement in the state of art.

Section II outlines the challenge of reconstructing the time delays from realistic data complete with systematics such as microlensing. The Gaussian process methodology is described in Sec. III, introducing the various correlation function terms and accounting for systematics. We test the method against blinded mock data, and real data from the literature, in Sec. IV, and conclude in Sec. V.

II. TIME DELAYED LIGHTCURVES

Fluxes received from an image at several times define a lightcurve, but the name is misleading since the data are not continuous but discrete, and the observations are often irregular and sparse and have measurement uncertainties. The best monitoring frequency may be every day or two, while long gaps of a few months occur due to seasonal visibility of regions of the sky from a single telescope. The cadence is often irregular, though ongoing wide area surveys such as Dark Energy Survey (DES [12]), Kilodegree Survey (KIDS [13]), and PanSTARRS [14], and in the future LSST [15], may have regular observations with periods of several days.

Apart from the sparseness, the data has photometric measurement noise. Most current observations come from small (1 meter) telescopes, and atmosphere, telescope, and detector noise all contribute. With wide field surveys, hundreds to thousands of time delay systems may be found, enabling choice of the cleanest for use as time delay distance probes. Since to obtain a time delay distance one must have a robust model of the lens mass distribution, galaxy lenses are preferred over cluster lenses due to less complex modeling. Depending on lens mass and geometry this implies time delays in the

range of a few to hundred days in general.

Comparing lightcurves from different images involves some form of cross-correlation, looking for the time delay between them. Straightforward cross-correlation techniques tend not to work well due to the noisiness and sparseness of the data, and extrinsic contributions (see, e.g., [16]). Instead of comparing noisy data with noisy data, regression techniques attempt to reconstruct the underlying true source variation and compare the image measurements to that. We employ Gaussian processes (GP) as the regression technique. See [17] for an example of its application to (non-lensed) supernova lightcurves.

In addition to measurement difficulties, astrophysical systematics contribute to the challenge of time delay estimation. Further time variations arise from microlensing caused by passage of substructure near to the line of sight. This affects images independently, breaking the (delayed) coherence between them, and can occur on all time scales. Short variations just add noise but long term variations disrupt the relation between the lightcurves for large portions of the data set and so can cause misestimation of the time delay. These long term variations are moderately smooth and some previous work has used low order polynomials or splines to represent them; we instead allow the data to determine their time scale.

Thus we have three elements entering into the light curves: the intrinsic variation that we want to measure, the observational noise, and the astrophysical microlensing systematic (in fact our formalism would allow multiple versions of the last two). The challenge of robust time delay estimation is to reconstruct phase shifts of a source with unknown intrinsic flux variation, for images with independent microlensing magnifications along their lines of sight, using noisy data with irregular temporal sampling. Figure 1 shows an example of real lightcurves from four images of quasar HE 0435-1223 measured by CosmoGrail [18]. Conventionally observations are reported in magnitudes (logarithmic flux units).

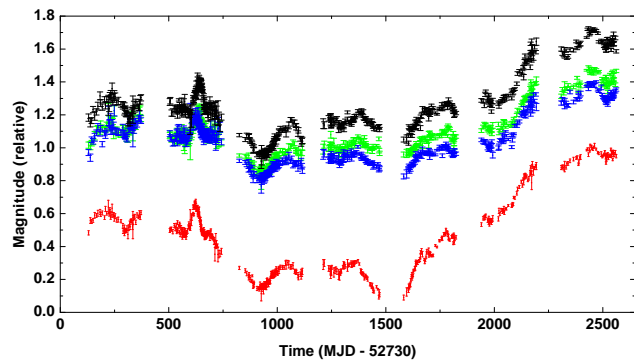


FIG. 1. Magnitudes (log flux) of four images of the quasar HE 0435-1223 are plotted vs time, with an arbitrary overall zeropoint.

III. TIME DELAY ESTIMATION

For reconstructing an intrinsic function from isolated, noisy data points, Gaussian processes offer a robust, substantially model independent statistical method with well defined error characterization. See [19] for a thorough discussion of GP from a statistical point of view. The basic idea is that the function is not parametrized, but rather the data are fit to a whole family of possible curves, given by a Gaussian distribution with a mean function and a covariance kernel between points.

The key choices are the form of the mean function (which ideally does not affect the final fit but in practice a poor mean function can lead to difficulties) and the covariance kernel, together with any hyperparameters used in those functions. There is a single GP representing the true source underlying all of the images plus the microlensing of a reference image. For a mean function we adopt a constant function, then allow hyperparameters for magnifications relative to the reference image. We try different reference images to test for robustness.

For the covariance kernel we adopt a Matern function with index $3/2$,

$$k(t_i, t_j) = \sigma^2 \left(1 + \frac{|t_i - t_j| \sqrt{3}}{l} \right) e^{-|t_i - t_j| \sqrt{3}/l}, \quad (1)$$

where t_i and t_j are measurement times, the hyperparameter σ adjusts the amplitude of the kernel and l functions as a correlation length. The Matern function is commonly used in statistics [19] and allows for greater roughness in the variation than another common choice, the squared exponential or Gaussian,

$$k(t_i, t_j) = \sigma^2 e^{-(t_i - t_j)^2 / (2l^2)}. \quad (2)$$

We will compare the results for these two kernels; generally we find that they work comparably well, with the Matern case often having somewhat smaller statistical errors and bias.

We include measurement noise and an additional nugget term $\sigma_n^2 \delta_{ij}$, which acts as a zero lag dispersion, i.e. the noise in a point process at a given time. This is distinct from the GP amplitude σ in that σ accounts for the global variations of the kernel whereas the nugget term σ_n accounts for the independent dispersion of the individual data points around the predicted GP value.

The microlensing systematic has been attempted to be addressed in the literature by multiplying the lightcurves by a quadratic polynomial or a cubic spline over short time spans or within an observing season. This restricts the allowed variations and has the potential to lead to bias in the reconstructed time delays or simply a failed fit. We remain within the GP framework, which does not impose a specific model or timescale for the microlensing, and account for the microlensing with a GP for each image (other than the reference one) with zero mean function and a squared exponential kernel of common

amplitudes σ_μ^2 and correlation lengths l_μ . To separate the microlensing GP from the quasar GP, we require a long correlation length l_μ (systems with the microlensing timescale comparable to the intrinsic variations are not useful for time delay measurement). We have investigated various choices of priors, for example $\pi(l_\mu) > 50$ days, $\pi(l_\mu) > \text{season}$, or $\pi(l_\mu) > 3l$; all give equivalent results.

In summary, the lightcurve predictions for our full GP regression take the form

$$\vec{y}_1 \sim GP_Q(\vec{\theta}_{\text{Qhp}}; t - t_1) \quad (3)$$

$$\vec{y}_2 \sim GP_Q(\vec{\theta}_{\text{Qhp}}; t - t_2) + GP_{\mu 2}(\vec{\theta}_{\mu\text{hp}}) + \Delta m_2 \quad (4)$$

$$\vec{y}_3 \sim GP_Q(\vec{\theta}_{\text{Qhp}}; t - t_3) + GP_{\mu 3}(\vec{\theta}_{\mu\text{hp}}) + \Delta m_3 \quad (5)$$

$$(6)$$

and so forth for each image, where $\vec{\theta}_{\text{Qhp}}$ is the hyperparameter vector for the quasar GP, $\vec{\theta}_{\mu\text{hp}}$ is for the microlensing GP, and Δm represents the magnification relative to the reference image 1.

The GP likelihood is [19]

$$2 \ln p(Y|\vec{\theta}) = -Y^T K^{-1} Y - \ln |K| - N_d \ln 2\pi, \quad (7)$$

where Y is the vector of magnitude data, with N_d the total number of data points, $\vec{\theta}$ represents the fit parameters, e.g. time delays, and K is the full kernel with $|K|$ being its determinant. The likelihood is maximized for the most likely values of the time delays and magnifications, which we find using the function minimizer routine Minuit [20] and have validated using a Monte Carlo analysis.

In principle, we can combine all lightcurves at once, compare two at a time, or any number of lightcurves. Simultaneous analysis of more than two curves allows a consistency check in the form of the triangle equality, e.g. $\Delta t_{AC} = \Delta t_{AB} + \Delta t_{BC}$, and is our baseline approach. Using more lightcurves also has the advantage of the leverage of more images on simultaneously constraining the underlying source light curve. Analysis using just a pair has fewer hyperparameters and may deliver smaller statistical errors, but at the risk of bias. We carry out cross-checks by trying different numbers of lightcurves in the analysis, finding that the results from the pair analyses can provide useful initial conditions to the simultaneous fit. One can also use portions of data, such as selected observation seasons, to cross check the consistency of the results or to reduce the impact of microlensing as has been done in the literature before. We find the results from our approach to be robust to the number of data points used in the analysis.

In summary, when fitting N lightcurves we have the $N - 1$ time delay parameters that are our goal, the $N - 1$ magnifications Δm , and the hyperparameters σ^2 , σ_n^2 , σ_μ^2 , l , l_μ .

IV. TESTS AND RESULTS

A. Blind mock data

To test the accuracy and robustness of the method we initially created blinded mock data sets. To preserve realistic sampling and data quality, one author took lightcurve data from one image of quasar HE 0435-1223, realized three new lightcurves using random Gaussian distributions with mean zero and standard deviation equal to the data errors, and shifted each of the resulting lightcurves vertically by various magnifications and horizontally by time delays. The shifted data were then resampled onto the original time sampling using linear interpolation. Another author, unaware of the simulated time delay and magnification values, was given the final data points with error bars and carried out the GP fit.

The results are shown in Table I, with the true values of 15.0 and 25.0 day delays recovered within the 68% confidence level. Several other tests with different time delays had similar results. Both Matern and squared exponential kernels work well. We find that the magnification and nugget terms are both important to include. Time delays are also tested for robustness by choosing different reference curves and different multiplicities (i.e. fitting for the AB time delay in isolation, or simultaneously fitting the GP to more than two lightcurves). Quoted values reflect the central values and uncertainties from the configuration that has the best reduced χ^2 and the smallest errors. These uncertainties are marginalized over all the other parameters and hyperparameters.

Kernel	Δt_{AB}	Δt_{AC}	Δt_{BC}
Matern	14.3 ± 0.8	25.1 ± 0.9	10.8 ± 0.9
Sq Exp	13.9 ± 1.3	25.8 ± 1.4	10.6 ± 0.7
Matern 2-curve	14.8 ± 1.0	25.1 ± 1.2	11.2 ± 1.0
Sq Exp 2-curve	15.0 ± 1.2	25.7 ± 1.4	12.0 ± 1.4

TABLE I. Blind analysis of time delays works for both Matern and squared exponential GPs, whether analyzing all lightcurves simultaneously (our standard approach) or in pairs (“2-curve”). The input to the simulation had $\Delta t_{AB} = 15.0$ days, $\Delta t_{AC} = 25.0$ days.

Figure 2 shows the 1D and 2D joint likelihood contours for the time delay parameters in the mock data case. As a comparison, these results are obtained using CosmoMC [21] as a generic Monte Carlo sampler, and are wholly consistent with the Minuit results. For all the parameters and hyperparameters we impose a very wide flat prior and let data decide their values. The only constraint is on the microlensing correlation length, which as discussed should not be too small and hence mix with the actual correlation length of the GP kernel.

A larger and more sophisticated series of data challenges is forthcoming as part of the LSST Dark Energy Science Collaboration strong lensing working group.

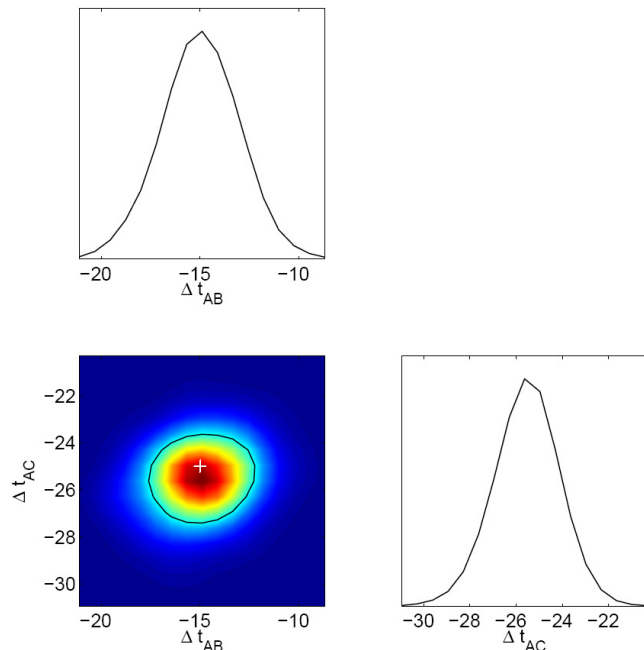


FIG. 2. Marginalized 1D and 2D likelihood contours are illustrated for the two time delays in the mock data case. The fiducial value is marked with a white plus sign.

B. Actual data

The second part of testing the GP method involves using public data sets from CosmoGrail and other literature sources [3, 4, 22–24] as inputs for time delay estimation. These results can then be compared to the literature results obtained using a variety of different methods.

We use the two sets of CosmoGrail lightcurves publicly available at [18], for quasars HE 0435-1223 and WFI J2033-4723, and the radio lightcurves of quasar B1608+656, courtesy of Chris Fassnacht. Table II compares the results we obtain from our baseline GP analysis using the Matern kernel with those published in the literature. The values are consistent with each other, with the GP analysis tending to have smaller errors. Note the true values of the time delays are not known, but the consistency offers an indication of robustness.

The GP analysis not only estimates the time delays, a key input for cosmography through time delay distances, but provides information on the intrinsic quasar variability, the variations around the best fit GP lightcurve, and the microlensing systematics through the hyperparameters such as the correlation lengths, GP amplitudes, and nugget.

We find that there is no significant correlation between the parameters. The nugget term is usually important and has a value comparable to the errors on the data points. We also find that including the microlensing term is useful even when there is no significant microlensing in the system.

The quasar HE 0435-1223 (Fig. 1) has a long observation period with distinct features in the intrinsic variability, making it fairly straightforward to compute the time delays. The bottom curve has significant microlensing variation which leads to large microlensing amplitude σ_μ . The microlensing correlation length (~ 700 days) is completely separated from the quasar GP correlation length (~ 100 days). There is strong agreement between our results, those of Literature 1 [3] that uses only the first two observation seasons, and those of Literature 2 [23]. Our uncertainties are often smaller by a factor of two.

The quasar WFI J2033-4723 has a relatively shorter observation time but distinct features in the light curves. There is no significant long-range microlensing and hence σ_μ is very small indicating that including microlensing terms may not be necessary (but this is not known a priori). Again, despite using several hyperparameters, our marginalized errors are comparable or smaller to results from [22].

The quasar B1608+656 (lightcurves shown in Fig. 3) is an example of a challenging system with large data gaps, relatively small intrinsic variability, and significant microlensing, all of which make it hard to estimate the time delays of its images. While we have successfully derived the time delays between all the images, including the cases not presented in the literature, the errors bars are relatively large. This is in part due to the featureless light curves (especially the bottom curve, D in Table II, which is almost flat) and also due to the fact that our errors are marginalized over other parameters. For example, fitting the nugget term increases the errors by at least a factor of two while its presence is relatively unimportant for this system.

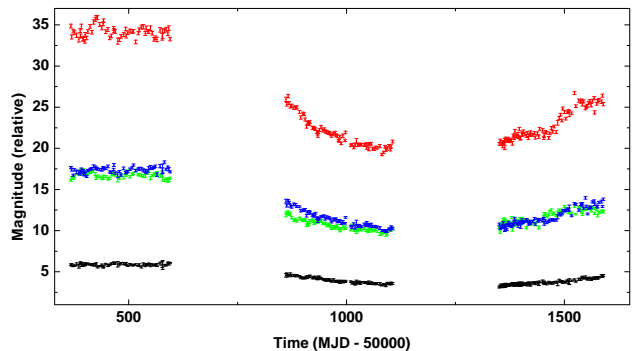


FIG. 3. Magnitudes (log flux) of four images of the quasar B1608+656 are plotted vs time, with an arbitrary overall zero-point.

V. CONCLUSIONS

Accurate estimation of strong lensing time delays is an essential element in the use of time delay distances as

Kernel	Δt_{AB}	Δt_{AC}	Δt_{AD}	Δt_{BC}	Δt_{BD}	Δt_{CD}
HE 0435-1223 GP	-9.6 ± 1.1	-1.5 ± 1.1	-14.0 ± 0.9	8.1 ± 1.1	-5.0 ± 1.1	-12.3 ± 1.1
HE 0435-1223 Lit(1) [3]	-8.4 ± 2.1	-0.6 ± 2.3	-14.9 ± 2.1	7.8 ± 0.8	-6.5 ± 0.7	-14.3 ± 0.8
HE 0435-1223 Lit(2) [23]	-8.8 ± 2.4	-2.0 ± 2.7	-14.7 ± 2.0	6.8 ± 2.7	-5.9 ± 1.7	-12.7 ± 2.5
WFI J2033-4723 GP	36.0 ± 1.5	-26.3 ± 1.7	–	-62.0 ± 2.3	–	–
WFI J2033-4723 Lit [22]	35.5 ± 1.4	$-27.1 \pm 4.1/-2.3$	–	?	–	–
B1608+656 GP	31.7 ± 2.1	-2.4 ± 2.2	-50.4 ± 6.9	-35.0 ± 4.0	-77.5 ± 7.1	-44.4 ± 5.4
B1608+656 Lit [24]	$31.5 \pm 2.0/-1.0$?	?	-36.0 ± 1.5	$-77.0 \pm 2.0/-1.0$?

TABLE II. Time delay estimations are compared between our GP analysis and values in the literature using different reconstruction methods. A question mark represents time delay estimates not provided by the literature, a dash indicates there is no fourth image.

a novel cosmological probe. The complementarity, substantially geometric nature, and disjoint systematics of this technique make its use a goal worth striving for.

We have explored Gaussian processes as a regression method that is effectively model independent and we demonstrated robust results for both blind mock data and actual literature data, in many cases reducing the uncertainties of the time delay estimations. Noisy data, gaps in the observations, and extrinsic microlensing variations can all be handled by the method.

Robustness arises not just from the technique itself, but the ability to use multiple lightcurves simultaneously, and test results against different combinations. Several possibilities exist for further improvement. One could weight the estimations derived from different combination of curves; one could remove unnecessary hyperparameters to reduce estimation uncertainty while checking that the best fit does not shift; and of course one could obtain better data. Forthcoming surveys will find many more suitable lensing systems, allowing choice of the cleanest or best observed (with low photometric uncertainties, better cadence with fewer gaps, etc.). Simulated data challenges will also provide important training

and assessment of the reconstruction method.

While time delay estimation is just one element in the development of strong lensing distances as a new cosmological probe, its improvement is key to this promising technique for mapping the Universe. Future work includes applying our GP reconstruction method to studies of lensed supernovae or other variable sources.

ACKNOWLEDGMENTS

We thank Chris Fassnacht for providing lightcurve data and Arman Shafieloo for helpful discussions. AH acknowledges the Berkeley Center for Cosmological Physics for hospitality. This work has been supported by World Class University grant R32-2009-000-10130-0 through the National Research Foundation, Ministry of Education, Science and Technology of Korea and the Director, Office of Science, Office of High Energy Physics, of the U.S. Department of Energy under Contract No. DE-AC02-05CH11231.

-
- [1] M. Oguri, ApJ 660, 1 (2007) [[arXiv:astro-ph/0609694](#)]
 - [2] S.H. Suyu, P.J. Marshall, R.D. Blandford, C.D. Fassnacht, L.V.E. Koopmans, J.P. McKean, T. Treu, ApJ 691, 277 (2009) [[arXiv:0804.2827](#)]
 - [3] F. Courbin et al, Astron. Astrophys. 536, A53 (2011) [[arXiv:1009.1473](#)]
 - [4] S.H. Suyu, P.J. Marshall, M.W. Auger, S. Hilbert, R.D. Blandford, L.V.E. Koopmans, C.D. Fassnacht, T. Treu, ApJ 711, 201 (2010) [[arXiv:0910.2773](#)]
 - [5] R. Fadely, C.R. Keeton, R. Nakajima, G.M. Bernstein, ApJ 711, 246 (2010) [[arXiv:0909.1807](#)]
 - [6] E.V. Linder, Phys. Rev. D 70, 043534 (2004) [[arXiv:astro-ph/0401433](#)]
 - [7] E.V. Linder, Phys. Rev. D 84, 123529 (2011) [[arXiv:1109.2592](#)]
 - [8] M. Tewes, F. Courbin, G. Meylan, [arXiv:1208.5598](#)
 - [9] M. Tewes et al, [arXiv:1208.6009](#)
 - [10] S.H. Suyu et al, ApJ 766, 70 (2013) [[arXiv:1208.6010](#)]
 - [11] W.H. Press, G.B. Rybicki, J.N. Hewitt, ApJ 385, 404 (1992)
 - [12] Dark Energy Survey Collaboration, [arXiv:astro-ph/0510346](#)
<http://www.darkenergysurvey.org>
 - [13] J.T.A. de Jong, G.A. Verdoes Kleijn, K.H. Kuijken, E.A. Valentin, Experimental Astron. 35, 25 (2013) [[arXiv:1206.1254](#)]
<http://kids.strw.leidenuniv.nl>
 - [14] N. Kaiser et al, Proc. SPIE 7733, 77330E (2010)
<http://pan-starrs.ifa.hawaii.edu>
 - [15] LSST Dark Energy Science Collaboration, [arXiv:1211.0310](#)
<http://www.lsst.org/lsst>
 - [16] L.V.E. Koopmans, A.G. de Bruyn, E. Xanthopoulos, C.D. Fassnacht, Astr. Astroph. 356, 391 (2000) [[arXiv:astro-ph/0001533](#)]
 - [17] A.G. Kim, ApJ 766, 84 (2013) [[arXiv:1302.2925](#)]
 - [18] <http://obswww.unige.ch/~tewes/cosmograil/public/lightcurves.php>
 - [19] C. E. Rasmussen & C. K. I. Williams, Gaussian Processes for Machine Learning, MIT Press (2006)

- www.GaussianProcess.org/gpml
- [20] <http://seal.web.cern.ch/seal/work-packages/mathlibs/minuit/home.html>
- [21] A. Lewis, S. Bridle, Phys. Rev. D 66, 103511 (2002) [[arXiv:astro-ph/0205436](#)]
- [22] C. Vuissoz et al, Astron. Astrophys. 488, 481 (2008) [[arXiv:0803.4015](#)]
- [23] C. S. Kochanek, N. D. Morgan, E. E. Falco, B. A. McLeod, J. N. Winn, J. Dembicky, and B. Ketzeback, Astrophys. J. 640, 47 (2006) [[arXiv:astro-ph/0508070](#)]
- [24] C. D. Fassnacht, E. Xanthopoulos, L. V. E. Koopmans, and D. Rusin, Astrophys. J. 581, 823 (2002) [[arXiv:astro-ph/0208420](#)]